

### **Remote Sensing Letters**



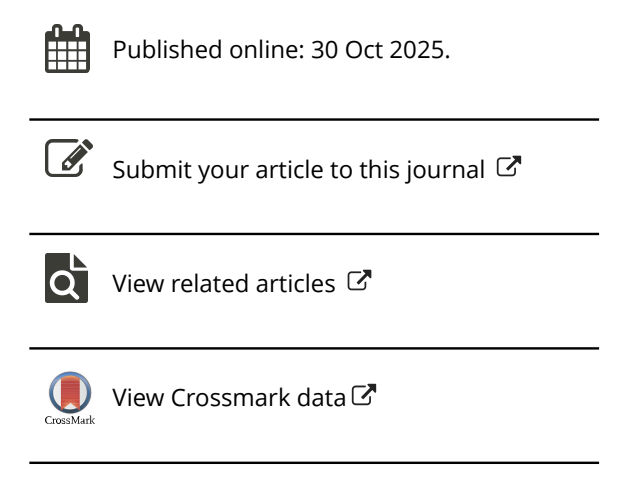
ISSN: 2150-704X (Print) 2150-7058 (Online) Journal homepage: www.tandfonline.com/journals/trsl20

# Improved S-Transform method in time-frequency domain for SAR RFI mitigation

Wenyi Fan, Puyan Xu, Xingwang Hu, Gaofeng Shu & Ning Li

**To cite this article:** Wenyi Fan, Puyan Xu, Xingwang Hu, Gaofeng Shu & Ning Li (2025) Improved S-Transform method in time-frequency domain for SAR RFI mitigation, Remote Sensing Letters, 16:12, 1414-1422, DOI: 10.1080/2150704X.2025.2579805

To link to this article: <a href="https://doi.org/10.1080/2150704X.2025.2579805">https://doi.org/10.1080/2150704X.2025.2579805</a>







## Improved S-Transform method in time-frequency domain for SAR RFI mitigation

Wenyi Fan<sup>a,b,c</sup>, Puyan Xu<sup>a,b,c</sup>, Xingwang Hu<sup>a,b,c</sup>, Gaofeng Shu pa,b,c and Ning Li pa,b,c

<sup>a</sup>College of Computer and Information Engineering, Henan University, Kaifeng, China; <sup>b</sup>Henan Engineering Research Center of Intelligent Technology and Application, Henan University, Kaifeng, China; <sup>c</sup>Henan Key Laboratory of Big Data Analysis and Processing, Henan University, Kaifeng, China

#### ABSTRACT

With the rapid development of modern communication technology, synthetic aperture radar (SAR) is encountering increasingly severe radio frequency interference (RFI), which significantly affects signal processing and image interpretation. Traditional timedomain and frequency-domain mitigation methods are insufficient to effectively identify RFI characteristics in complex environments. Consequently, time-frequency transformation techniques, which integrate both time and frequency information, have become the key in addressing these issues, especially in wideband interference mitigation. The short-time Fourier transform (STFT) is commonly employed due to its simplicity and efficiency, yet it is limited by time-frequency resolution. While the S-transform achieves higher time-frequency resolution, its application in RFI mitigation is still limited by low execution efficiency and poor time-frequency concentration. To address these issues, an improved S-transform method in time-frequency domain for SAR RFI mitigation is proposed in this article. This method primarily focuses on the impact of time-frequency transformation itself on RFI mitigation. By optimizing the window parameters of the S-transform, it can better adapt to abrupt changes in the signal, achieving improved timefrequency resolution and concentration. The experimental results based on simulated and measured SAR data confirm the effectiveness and superiority of the proposed method.

#### **ARTICLE HISTORY**

Received 26 December 2024 Accepted 16 October 2025

#### **KEYWORDS**

SAR; RFI mitigation; STFT; S-transform

#### 1. Introduction

Synthetic aperture radar (SAR) is an active microwave sensor that can track the ground at any time, regardless of weather or atmospheric conditions. However, the rapid development of modern communications has made radio frequency interference (RFI) in SAR increasingly complex. In this context, time-frequency transformation plays a key role in RFI feature extraction by combining time and frequency information, making time-frequency domain mitigation a primary approach for handling RFI in complex electromagnetic environments. However, most time-frequency domain RFI mitigation studies (Han et al. 2022; Su et al. 2017) focus on methods applied after time-frequency transformation, while

the potential impact of the transformation itself on RFI mitigation effectiveness was often neglected. Therefore, this article focuses on the time-frequency transformation method itself to enhance RFI mitigation effect.

Time-frequency transformation decomposes one-dimensional signals into the timefrequency domain to reveal localized features. Time-frequency transformation techniques commonly employed include the short-time Fourier transform (STFT) (Han et al. 2022), Wavelet Transform (WT) (S. Zhang et al. 2011), S-transform (Stockwell, Mansinha, and Lowe 1996), and Wigner-Ville Distribution (WVD) (Boudreaux-Bartels and Parks 1986). STFT and WT are efficient and easily invertible, but their resolution is limited by the uncertainty principle. The WVD provides high resolution, but suffers from cross-term RFI. The S-transform combines the strengths of STFT and WT, offering frequency-dependent resolution. However, the S-transform suffers from low efficiency and poor time-frequency concentration, limiting its application in RFI mitigation.

Aiming at the above issues, an improved S-transform method for SAR RFI mitigation is proposed. Firstly, a composite indicator (H. Zhang and Li 2024) is employed to detect and mark pulses containing RFI. Secondly, a window parameter optimized S-transform is constructed for time-frequency domain notch filtering. Finally, the processed pulses are combined with unmarked data to form new RFI-free echo data. The effectiveness of the proposed method is displayed by simulated and measured experiments.

#### 2. Related work

#### 2.1. RFI signal model

SAR systems are affected by RFI in complex electromagnetic environments. Each echo can be modelled as a one-dimensional time series, and the RFI-contaminated form is given by:

$$X(\tau, \eta) = S(\tau, \eta) + I(\tau, \eta) + N(\tau, \eta)$$
(1)

 $X(\tau,\eta)$  denotes the received echo signal, where  $S(\tau,\eta)$ ,  $I(\tau,\eta)$  and  $N(\tau,\eta)$  represent the useful signal, RFI, and system noise.  $\tau$  and  $\eta$  denote the range direction time unit and azimuth direction time unit, respectively. RFI can be classified as point frequency, frequency-modulated and narrowband amplitude-modulated based on real data analysis.

#### 2.2. S-transform

The S-transform achieves dynamic time-frequency resolution via a frequency-dependent Gaussian window. In the S-transform, the window width is inversely proportional to frequency and affects resolution. Narrow windows at high frequencies improve time resolution, whereas wider windows at low frequencies enhance frequency resolution. The S-transform of the continuous signal x(t) can be represented as:

$$S_{x}(\tau, f) = \int_{-\infty}^{\infty} x(t)w(t - \tau)\exp(-j2\pi ft)dt$$
 (2)

where f denotes the frequency variable, both  $\tau$  and t represent time variables. It should be noted that  $\tau$  is used to control the position of the window function along the time axis. The window function w(t,f) is frequency-dependent, as shown below:

$$w(t,f) = \frac{|f|}{\sqrt{2\pi}} exp\left(-\frac{t^2f^2}{2}\right) \tag{3}$$

Based on the energy conservation and reversibility properties of the S-transform under specific conditions, the original signal is recovered without loss by means of the following inverse transform:

$$x(t) = \int_{-\infty}^{\infty} S_x(\tau, f) exp(j2\pi ft) d\tau df$$
 (4)

where  $\exp(j2\pi ft)$  serves as the phase factor for reconstructing the time-domain signal.

#### 3. Methodology

To overcome the limitations of the S-transform in RFI mitigation, an improved S-transform method in time-frequency domain for SAR RFI mitigation is proposed in this article. A composite indicator is employed to detect and mark pulses containing RFI, reducing subsequent workload and improving overall efficiency. Simultaneously, window parameter optimization enhances time-frequency resolution and concentration, enabling clearer RFI boundaries and improved signal separation. The specific process for optimizing the window parameters is as follows:

Firstly, the amplitude spectrum of the original signal x(t) is calculated and subsequently smoothed and normalized to obtain the  $X_{\text{norm}}(f)$ .

$$X(f) = smooth\{|FT[x(t)]|\}$$
(5)

$$X_{\text{norm}}(f) = \frac{X(f)}{\max(|X(f)|)} \tag{6}$$

where FT denotes the Fourier transform, and smooth denotes the smoothing operation.

Then, the  $X_{\text{norm}}(f)$  is scaled to an appropriate range using the parameter r, which allows the amplitude to remain within a reasonable interval, thereby facilitating the subsequent calculation of the window function.

$$X_{r}(f) = [rX_{\text{norm}}(f)] + 1 \tag{7}$$

Subsequently, the window parameter p(f) is calculated based on frequency variations to achieve a better alignment with the varying frequency components of the signal.

$$p(f) = \frac{N_r}{2X_r(f)} \tag{8}$$

where  $N_r$  is defined as the number of range-direction sampling points. The optimized window parameters improve the time – frequency resolution and concentration of the signal to some extent, although there remains room for further enhancement.

Subsequently, parameters  $\alpha$  and  $\beta$  are introduced to further optimize the window parameter p(f), forming the adjustment parameters  $\sigma'$  for the improved S-transform.

$$\sigma' = \frac{[p(f)]^{\beta}}{\alpha} \tag{9}$$

The optimized window function w'(t, f) can be represented as:

$$w'(t,f) = \frac{a}{[p(t)]^{\beta}\sqrt{2\pi}} exp\left(-\frac{a^2t^2}{2[p(t)]^{2\beta}}\right)$$
 (10)

The optimized window function can distinguish different frequency components based on the amplitude of the real signal. Moreover, the flexibility of the transformation process and time-frequency concentration capability are enhanced by introducing adjustable parameters  $\alpha$  and  $\beta$ , allowing for more effective separation of various components in non-stationary signals.

The workflow of the proposed RFI mitigation method based on the aforementioned RFI detection method and the optimized S-transform with window parameters, is illustrated in Figure 1. The procedure is divided into four steps: RFI detection, time – frequency transformation, notch filtering, and inverse transformation. Notably, the inverse transformation is performed in accordance with Equation (4) and employs the same window function w'(t,f) used in the time – frequency transform to ensure accurate reconstruction of the original signal.

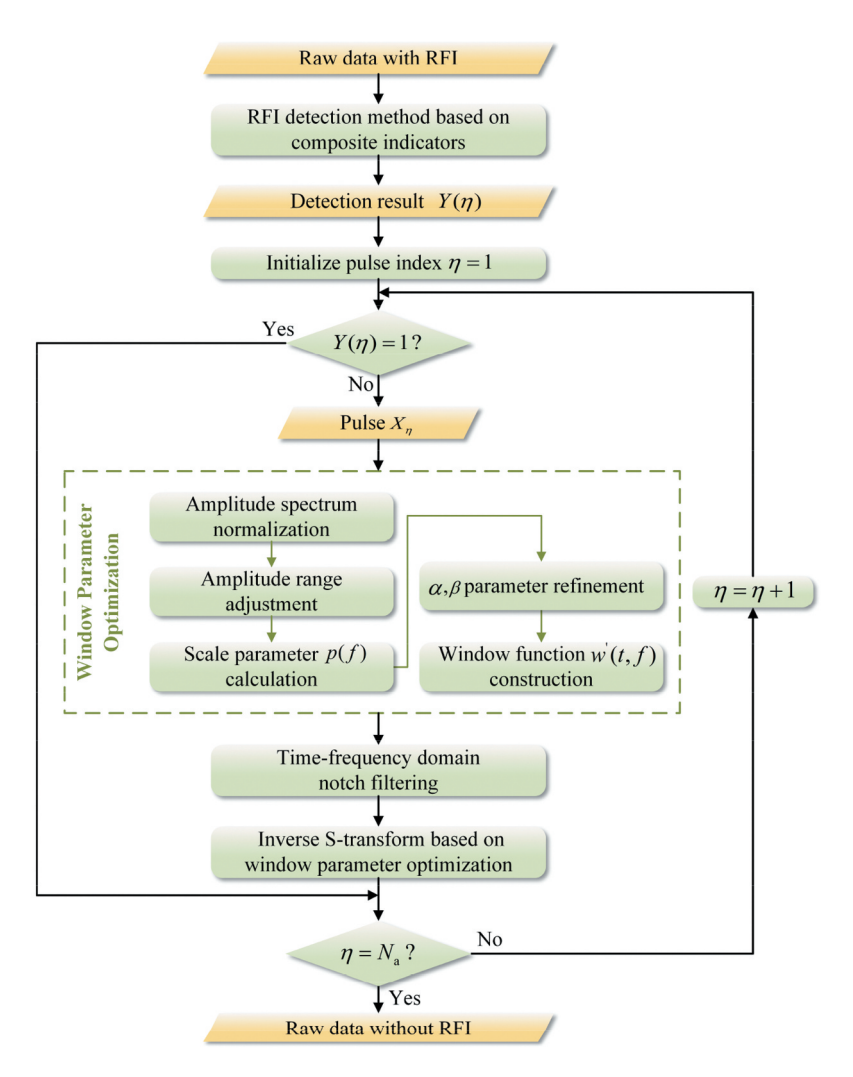


Figure 1. Flowchart of the proposed method.  $N_a$  denotes the number of sampling points in the azimuth direction.

#### 4. Experimental results

#### 4.1. Simulated data experimental results

To verify the proposed method's robustness, two types of RFI are added to raw Sentinel-1A data under different signal to interference plus noise ratio (SINR) conditions in simulation experiments. To evaluate its effectiveness, the proposed method is compared with RFI mitigation methods based on STFT and S-transform.

Figure 2 shows the time-frequency diagram of a pulse in the simulated data. As seen, the S-transform with optimized window parameters significantly improves time-frequency resolution, enhances the concentration of the RFI signal, facilitates more precise localization, and strengthens support for subsequent RFI mitigation. The RFI mitigation results of the three methods are shown in Figure 3, with a magnified view of the region of interest in the red box. Under the same SINR conditions, the proposed method preserves clear road and building details with minimal signal loss, effectively ensuring signal integrity. Additionally, the RFI over the sea is nearly eliminated, maximizing RFI mitigation.

The Rényi entropy, root mean square error (RMSE) (Lv et al. 2023) and running time are employed as evaluation metrics in this article. As shown in Tables 1 and 2, the improved S-transform exhibits higher time-frequency resolution and concentration, and the proposed method achieves superior interference mitigation performance, effectively eliminating RFI while preserving signal integrity. Moreover, the proposed method is more efficient than the S-transform-based method, but slower than the STFT-based method. Therefore, it is better suited for high-precision RFI mitigation.

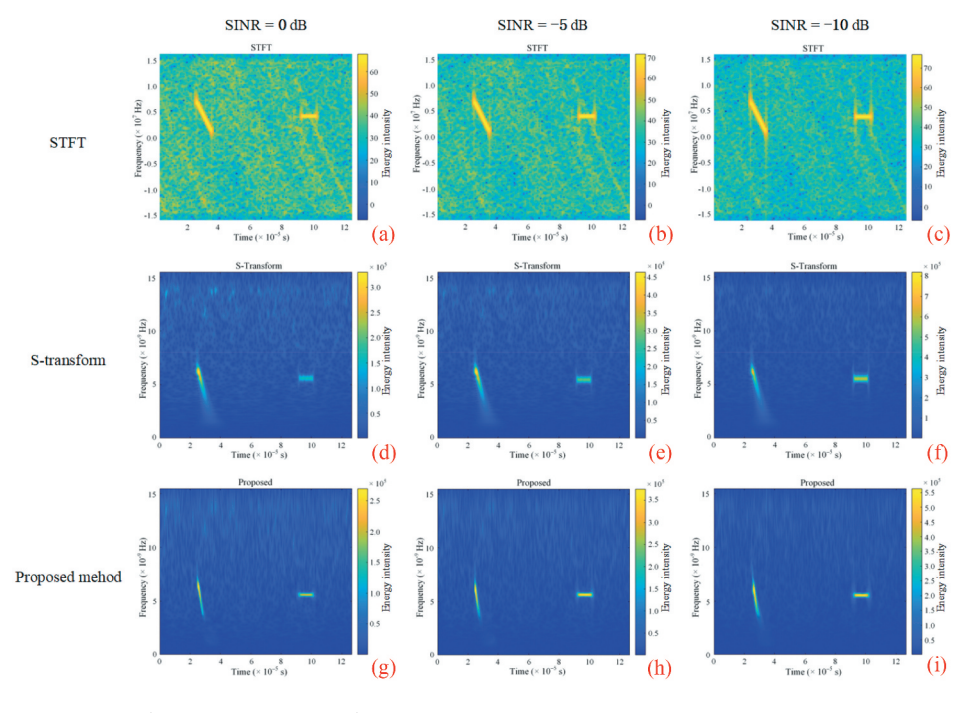


Figure 2. Time-frequency diagram of a pulse in the simulated data.

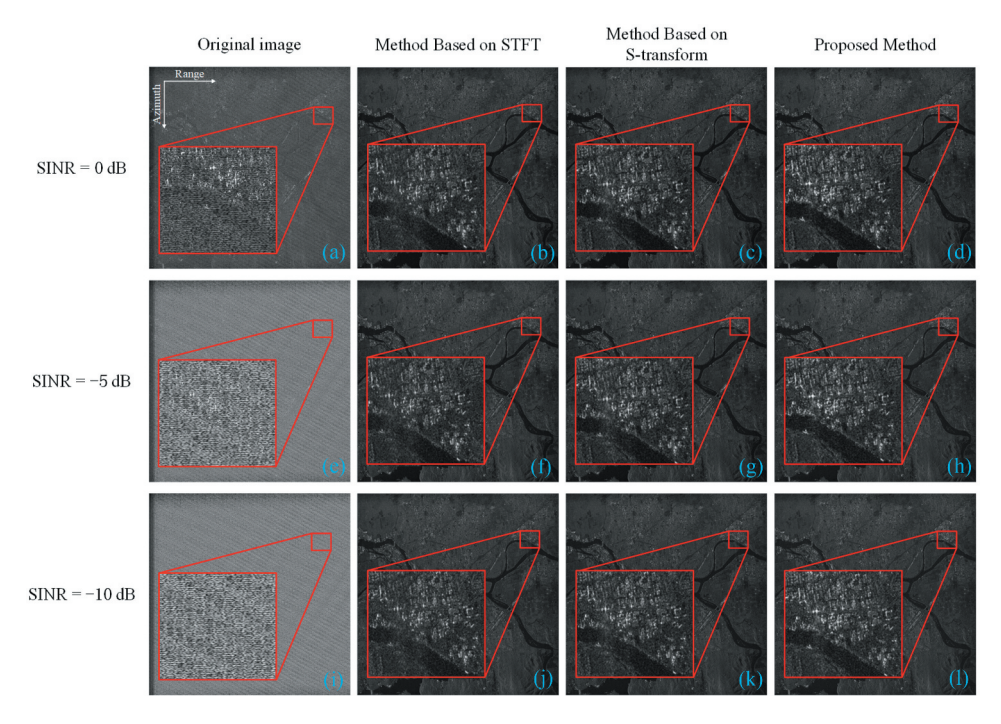


Figure 3. Performance comparison of interference mitigation methods with simulated data.

Table 1. Rényi entropy of time-frequency transform methods in simulated data.

SINR (dB)	STFT	S-transform	Improved S-transform
0	17.8490	14.4951	12.7364
<b>-</b> 5	18.2253	14.7131	13.0861
-10	18.9441	15.3027	13.7830

Note. bold values emphasize the best evaluation metrics in the experiments.

Table 2. RMSE of different RFI mitigation methods.

SINR (dB)	Method Based on  Method Based on STFT S-transform Proposed Method		
0	0.2664	0.2491	0.2069
-5	0.3016	0.2868	0.2586
-10	0.3902	0.3640	0.3145
Running Time (s)	62.5483	2923.3415	1213.4189

Note. bold values emphasize the best evaluation metrics in the experiments.

#### 4.2. Measured data experimental results

The measured data used is the raw C-band Sentinel-1A data with RFI obtained on 18 February 2022. As seen in Figure 4(d)-(f), the proposed method performs best in terms of time-frequency resolution and concentration. The quantitative results in Table 3 provide further validation of this conclusion. The imaging results after

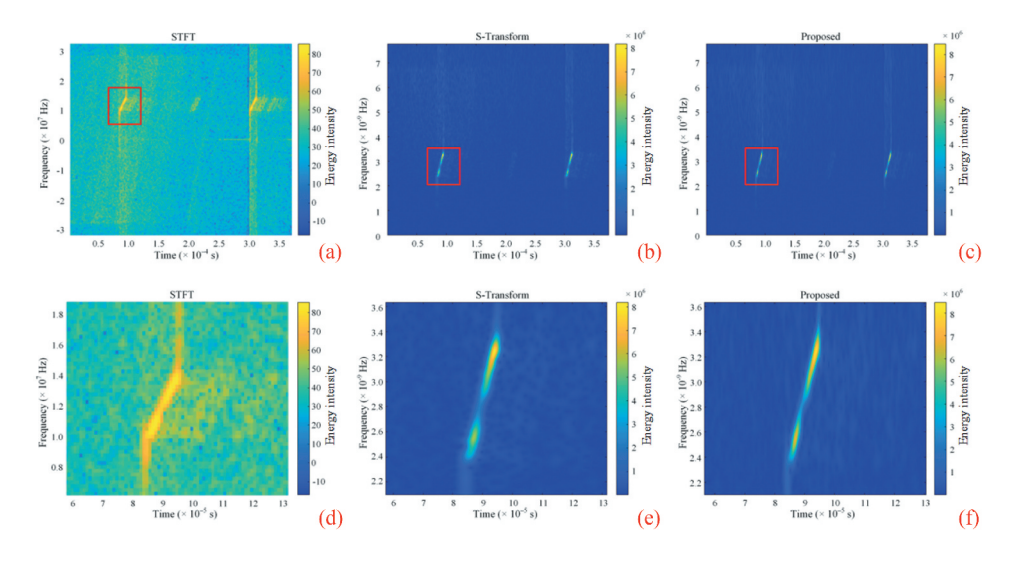


Figure 4. Time-frequency diagram of a pulse in the measured data. (d-f) The region of interests (ROIs) in (a-c) with red box.

Table 3. Rényi entropy of time-frequency transform methods in measured data.

Method	STFT	S-transform	Improved S-transform
Rényi entropy	18.3271	13.2596	11.9046

Note. bold values emphasize the best evaluation metrics in the experiments.

Table 4. Evaluation indicators of different RFI mitigation methods.

	Method Based on			
Method	Method Based on STFT	S-transform	Proposed Method	
Gray Entropy	2.5830	2.9516	3.8012	
Average Gradient	2027.1317	2669.3245	3223.6405	
Running Time (s)	161.2996	7592.8190	3151.1007	

Note. bold values emphasize the best evaluation metrics in the experiments.

applying different RFI mitigation methods are shown in Figure 5. As shown in the enlarged view, the proposed method demonstrates better performance in RFI mitigation and signal preservation. The white RFI streaks are nearly eliminated, and details in the RFI-free areas, such as roads and buildings, remain sharp and well-defined.

To comprehensively compare the performance of different RFI mitigation methods, this article uses grey entropy (Tang, Deng, and Zheng 2022), average gradient (AG) (Fan et al. 2019), and running time as metrics. As shown in Table 4, the proposed method achieves higher grey entropy and AG than the other two methods, indicating its effectiveness in removing RFI while better preserving the integrity of useful signals.

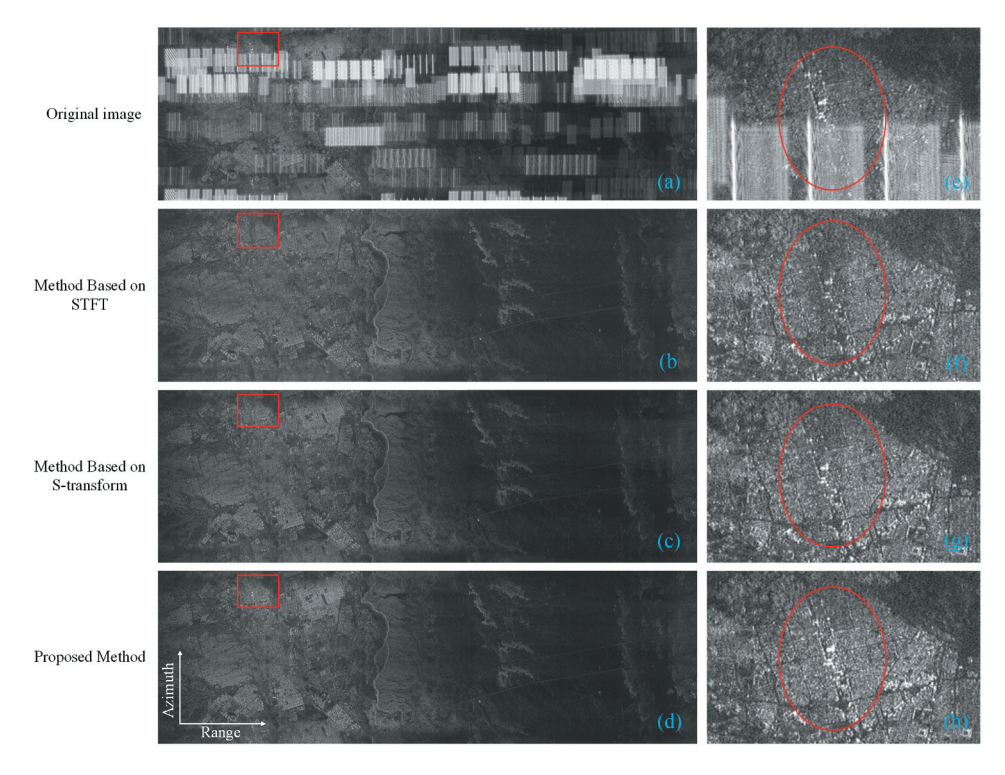


Figure 5. Performance comparison of interference mitigation methods with measured data. (e-h) ROIs in (a-c) with red box. Note. The red ellipses in parts (e) to (h) indicates the key contrast area.

#### 5. Conclusion

This article proposes an improved S-transform method for SAR RFI mitigation. By detecting and tagging RFI-contaminated pulses in advance, the method improves efficiency. Moreover, window parameter optimization further enhances time-frequency resolution and concentration. Experimental results show that the proposed method effectively mitigates RFI while preserving signal integrity, and significantly improves efficiency over traditional S-transform-based methods. Notably, when the data contains a high proportion of RFI pulses, the computational efficiency improvement of the proposed method is limited, and the window parameter optimization process exhibits inherent parameter sensitivity. This method can be widely applied to image processing in SAR systems and also provides new ideas for subsequent RFI mitigation research.

#### **Disclosure statement**

No potential conflict of interest was reported by the author(s).



#### **ORCID**

Gaofeng Shu (b) http://orcid.org/0000-0002-7098-7029 Ning Li (b) http://orcid.org/0000-0002-4358-6449

#### **Data availability statement**

The code and data that support the findings of this study are available from the authors upon reasonable request.

#### References

- Boudreaux-Bartels, G., and T. Parks. 1986. "Time-Varying Filtering and Signal Estimation Using Wigner Distribution Synthesis Techniques." *IEEE Transactions on Acoustics, Speech & Signal Processing* 34 (3): 442–451. https://doi.org/10.1109/TASSP.1986.1164833.
- Fan, W., F. Zhou, M. Tao, X. Bai, P. Rong, S. Yang, and T. Tian. 2019. "Interference Mitigation for Synthetic Aperture Radar Based on Deep Residual Network." *Remote Sensing* 11 (14): 1654. https://doi.org/10.3390/rs11141654.
- Han, W., X. Bai, W. Fan, L. Wang, and F. Zhou. 2022. "Wideband Interference Suppression for SAR via Instantaneous Frequency Estimation and Regularized Time-Frequency Filtering." *IEEE Transactions on Geoscience & Remote Sensing* 60:1–12. https://doi.org/10.1109/TGRS.2021. 3098783.
- Lv, Z., H. Fan, Z. Chen, J. Qiu, M. Ren, and Z. Zhang. 2023. "Mitigate the lfm-Prfi in SAR Data: Joint Down-Range and Cross-Range Filtering." *IEEE Transactions on Geoscience & Remote Sensing* 61:1–18. https://doi.org/10.1109/TGRS.2023.3265774.
- Stockwell, R. G., L. Mansinha, and R. P. Lowe. 1996. "Localization of the Complex Spectrum: The S Transform." *IEEE Transactions on Signal Processing* 44 (4): 998–1001. https://doi.org/10.1109/78. 492555.
- Su, J., H. Tao, M. Tao, L. Wang, and J. Xie. 2017. "Narrow-Band Interference Suppression via rpca-Based Signal Separation in time–Frequency Domain." *IEEE Journal of Selected Topics in Applied Earth Observations & Remote Sensing* 10 (11): 5016–5025. https://doi.org/10.1109/JSTARS.2017. 2727520.
- Tang, Z., Y. Deng, and H. Zheng. 2022. "RFI Suppression for SAR via a Dictionary-Based Nonconvex Low-Rank Minimization Framework and Its Adaptive Implementation." *Remote Sensing* 14 (3): 678. https://doi.org/10.3390/rs14030678.
- Zhang, H., and N. Li. 2024. "Composite Indicator for Detecting and Localizing Time-Varying RFI in SAR Raw Data." *IEEE Transactions on Geoscience & Remote Sensing* 62:1–14. https://doi.org/10.1109/TGRS.2023.3345151.
- Zhang, S., M. Xing, R. Guo, L. Zhang, and Z. Bao. 2011. "Interference Suppression Algorithm for SAR Based on time–Frequency Transform." *IEEE Transactions on Geoscience & Remote Sensing* 49 (10): 3765–3779. https://doi.org/10.1109/TGRS.2011.2164409.